Failure Mechanism of Columns of Existing R/C Building Damaged during the 2007 Niigata Chuetsu-Oki Earthquake

Daisuke Kato & Katsushi Yoshizawa
Department of Civil Engineering and Architecture, Niigata University, Japan

Tetsuo Nagahashi
SU Design Office, Niigata, Japan

Yukiko Nakamura
Department of Architecture, Chiba University, Japan

SUMMARY

The school building suffered from a great deal of damage during the 2007 Chuetsu-Oki Earthquake. The previous study revealed that the anticipated design failure modes of most of the columns of the building were flexure although most of them actually failed in shear. In order to study the reason a parametric study was also conducted and it was concluded that the diagonal crack generated from cut off point caused shear failure in these columns. In this study static loading tests were conducted varying the length of cut off bars and the presence of spandrel walls. Main conclusions were as follows; (1)The deformation capacity of a column with cut off bars degraded tremendously on condition that the yielding hinge location was cut off point and the inclination angle of diagonal cracks generated from the cut off point was approximately 50~60 degree. (2)The effect of presence of spandrel walls on deformation capacities was small.

Keywords: reinforced concrete, column, earthquake damage, cut off bar, shear failure

1. INTRODUCTION

The Niigata Chuetsu-Oki Earthquake generated with the epicenter depth of 17km on July 16, 2007. An earthquake scale was M6.8 and the maximum seismic intensity recorded upper 6 on the Japanese intensity scale in Nagaoka city, etc. The elementary school building investigated was a 3-story reinforced concrete (R/C) building built in 1963 (referred as S-building) in Oguni town of Nagaoka city.

S-building damaged moderately during the earthquake. The previous study (Nagahashi et al. 2009, Kato and Nagahashi 2011) revealed that the anticipated design failure modes of most of the columns of the building were flexure although most of them actually failed in shear. In order to study the reason why the columns failed in shear rather than in flexural, a parametric study was conducted, paying attention to parameters including the strength of concrete, hoop spacing and subjected axial force. From these studies it could be concluded that for 1st floor columns it was not impossible to explain that the gap between calculation and observation was caused by the fluctuation of concrete strength, hoop effects and subjected axial force, etc. However for 2nd floor columns it was impossible to explain the gap using these parameters.

The reason of this gap was presumed that the crack generated at the cut off point developed into the column end diagonally and the diagonal crack reduced the shear strength of the column. Figure 1.1 shows reinforcement of 2F-A4 column (column number 4 of A frame of the 2nd floor) and the observed damage. Figure 1.2 shows isometric drawing and the section of the reinforcement of 2F-A4 column. It must be pointed out that α bar and β bar represent anchorage portion of longitudinal reinforcement of the 1st floor column just under 2F-A4 column. Length between the cut off point and the top of spandrel wall is 570mm for α bar and 170mm for β bar.

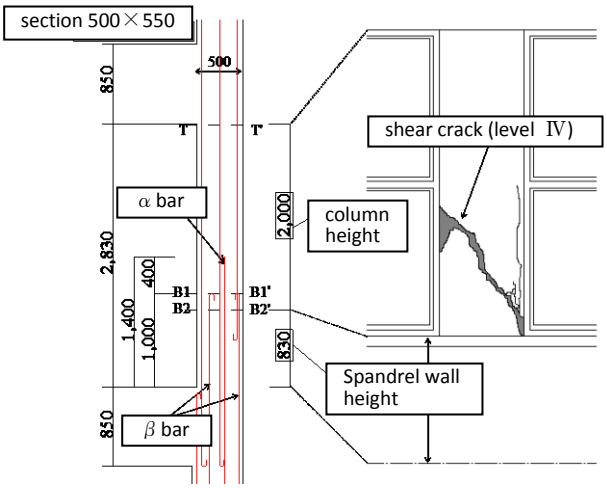

(a)Reinforcement (span direction) (b)Damage (ridge direction)

Figure 1.1. Reinforcing arrangement of 2F-A4 column and the observed damage

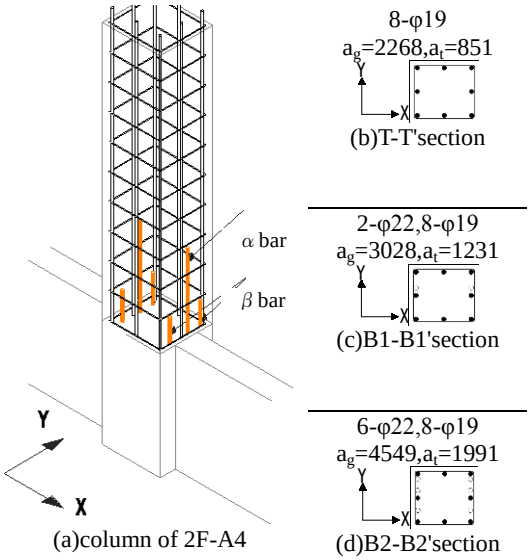

(a)column of 2F-A4

Figure 1.2. Reinforcing arrangement and the section of 2F-A4 column

This phenomenon analogizes to failure mechanism of pier columns with cut off main bars. But the difference is that cut off bars are necessary in case of pier columns whereas cut off bars are not necessary in case of S-building, which means cut off bars of S-building are the anchorage portion of 1st floor column just under the objective column.

2. OUTLINE OF EXPERIMENT

2.1 Test specimens

In order to demonstrate the presumption, static loading tests of six R/C columns were conducted. Table 2.1 shows properties of specimens. Figure 2.1 shows reinforcement of specimens with cut off bars. Main variables were the presence of cut off bars, the amount and length of cut off bars and the presence of spandrel walls. Specimen SIM-0 represented the basic specimen without cut off bars. The amount and the length of cut off bars are the most important factor to determine the hinge location; i.e. column end or cut off point, which have a strong influence on the failure mechanism of columns. Three specimens SIM-L, SIM-S and SIM-LL were specimens with cut off bars varying the amount

and the length. The cut off bars of specimen SIM-L and SIM-S represented those of α bars and β bars only in Figure 1.2, respectively. On the other hands cut off bars of specimen SIM-LL represented both α bars and β bars. But it must be noted the length of β bars were assumed to be same as that of α bars.

By the way the presence of spandrel wall might have had a deal of influence on the confinement of column end portion. From this view point two specimens with spandrel walls were tested. Specimen SIM-LL-k was a companion specimen with specimen SIM-L, which means that the difference of these two specimens was the presence of spandrel walls. Similarly specimen SIM-SS-k was a companion specimen with specimen SIM-S. But it must be noted the amount of cut off bars were different between these two specimens.

Table 2.2 shows calculated strength and failure modes of specimens, which were obtained according to the AIJ Structural Design Guidelines for reinforced Concrete Buildings (Architectural Institute of Japan (1994)). The table shows that all specimens were designed to fail in flexure but the position of the yielding hinge point differed according to the amount and the length of cut off bars.

Table 2.1. Properties of specimens

specimen	SIM-0	SIM-S	SIM-L	SIM-LL	SIM-LL-k	SIM-SS-k
section width (mm)	245					
section depth (mm)	270					
column inner height (mm)	980					
main bar (strength(N/mm^2))	6-ϕ9 (326)			6-ϕ9 (325)		
hoop (strength(N/mm^2))	2-ϕ4 (461)			2-ϕ4 (487)		
hoop spacing(mm)	98					
hoop detail	with 90 degree hook					
hoop p_w (%)	0.10					
cutoff bar (strength(N/mm^2))	-	2-ϕ13 (315)		6-ϕ13 (320)		
cut off length(mm)	-	120	280	280	280	120
concrete (N/mm^2)	18.0			24.7		
main loading	lateral loading (axial load 80 (kN))					
post loading	residual axial loading					
spandrel wall heigh (mm)	-	-	-	-	220	

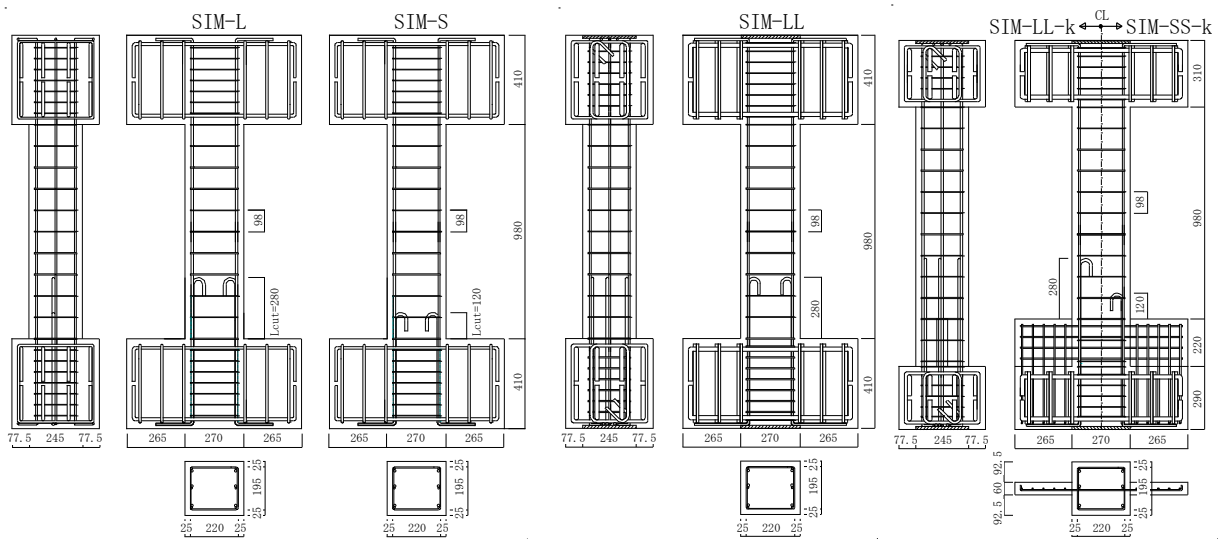

(a)SIM-L (b)SIM-S (c)SIM-LL (d)SIM-LL-k & SIM-SS-k

Figure 2.1. Specimens and reinforcement

Table 2.2. Caluculated strength and failure mode

specimen	SIM-0	SIM-S	SIM-L	SIM-LL	SIM-LL-k	SIM-SS-k
flexural crack strength at bottom(kN)	17.9	18.7	18.7	20.0	20.0	20.0
flexural crack strength at cutoff point(kN)	-	20.4	25.1	26.9	26.9	21.9
shear crack strength (kN)	41.6	41.6	41.6	47.0	47.0	47.0
flexural yielding strength at bottom (kN)	47.9	57.4	57.4	77.1	77.1	77.1
flexural yielding strength at cutoff point (kN)	-	54.6	67.1	67.7	67.7	55.1
shear strength (kN)	74.1	74.1	74.1	79.8	79.8	79.8
calculated maximum strength (kN)	47.9	54.6	57.4	67.7	67.7	55.1
calculated failure mode	flexure					
calculated yielding hinge location	bottom	cutoff point	bottom	cutoff point	cutoff point	cutoff point

2.2 Loading method

The loading was divided into two parts; i.e. main-loading and post-loading. The main loading represented lateral loading. The lateral loading tests were conducted using two vertical jacks to make the deformation at the top and the bottom of test specimens symmetrical. Specimens were subjected to lateral load reversals using one horizontal jack under a scheduled constant axial load of 80 kN shown in Figure 2.2. The lateral load was reversed twice for each drift angle of 1/200, 2/200, 3/200, 4/200, 6/200, 8/200, 12/200 and 16/200 rad. Each cycle was performed twice and the loading was terminated when the restoring force degraded to 80% of the maximum strength.

Authors have studied on axial load capacities and residual axial load capacities of R/C columns (Kato et al. 2009, Kato and Nakamura 2011). From this view point after the termination of lateral loading test an axial compression load was applied as a post-loading to all specimens. The axial compression load was applied after returning their displacement to zero and the displacement was maintained during the post-loading.

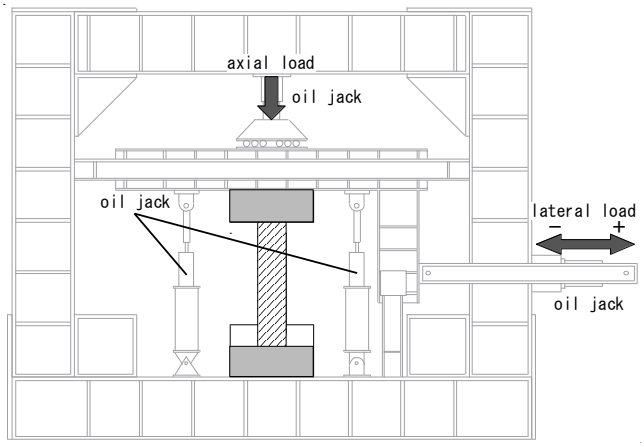

Figure 2.2. Loading setup

3. TEST RESULTS

Table 3.1 shows experimental results on flexural crack, diagonal crack, maximum strength and deformation capacity of all specimens. Figure 3.1 shows crack patterns of specimens at maximum strength. At maximum strength cracks were generated at the cut off point in all specimens except for specimen SIM-0 without cut off bars and the cracks were developed into the column end diagonally, which were similar to the actual damage during the earthquake. After maximum strength the diagonal cracks reduced the shear strength of the columns. After the termination of lateral loading test an axial

compression load was applied as the post-loading. Observed residual axial load capacities, which were defined as maximum load during the post-loading, were shown in the bottom two lines of Table 3.1. The residual axial load capacity ratios were obtained by dividing the maximum load by $bD\sigma_B$.

Figure 3.2(a)~(f) show lateral load- lateral drift angle relationship. In the figure circle marks represent the deformation capacities which were the loss points of design lateral load defined as the point where the restoring force degraded to 80% of the maximum strength. The basic specimen SIM-0 without cut off bars showed ductile behavior, the deformation capacity of which was more than 0.06 rad. Specimen SIM-S and SIM-L showed almost the same behavior as specimen SIM-0. Note that the yielding hinge location of longitudinal reinforcement of SIM-S was at the cut off point and that of SIM-L was the bottom of the column. On the other hand specimen SIM-LL showed brittle behavior which was caused by yielding of hoop reinforcement and the deterioration of shear resistance between the diagonal crack surfaces around the cut off point just after the specimen reached the maximum strength.

Specimen SIM-LL-k with spandrel walls showed almost the same behavior as specimen SIM-LL, which was the companion specimen without spandrel walls. However the maximum strength of specimen with spandrel walls was a little bit smaller comparing to that of specimen without spandrel walls. On the other hand specimen SIM-SS-k with spandrel walls also showed almost the same behavior as specimen SIM-S, which was the companion specimen without spandrel walls. However the maximum strength of specimen with spandrel walls was a little bit smaller comparing to that of specimen without spandrel walls.

Specimen SIM-LL-k with spandrel walls showed almost the same behavior as specimen SIM-LL, which was the companion specimen without spandrel walls. However the maximum strength of specimen with spandrel walls was a little bit smaller comparing to that of specimen without spandrel walls. On the other hand specimen SIM-SS-k with spandrel walls also showed almost the same behavior as specimen SIM-S, which was the companion specimen without spandrel walls. However the maximum strength of specimen with spandrel walls was a little bit smaller comparing to that of specimen without spandrel walls.

Table 3.1. Experimental results

specimen	SIM-0	SIM-S	SIM-L	SIM-LL	SIM-LL-k	SIM-SS-k
drift angle at flexural crack (rad)	0.0036	0.0041	0.0021	0.0015	0.0008	0.0004
drift angle at diagonal crack (rad)	-	0.0082	0.0050	0.0041	0.0020	0.0012
drift angle at flexural yielding (rad)	0.0050	0.0062	0.0096	0.0098	0.0093	0.0098
drift angle at hoop yielding (rad)	-	-	-	0.014	-	-
maximum strength (positive loading) (kN)	40.2	48.0	48.0	57.3	47.5	44.1
maximum strength (negative loading) (kN)	-43.6	-43.4	-51.7	-55.9	-51.2	-46.3
deformation capacity(*) (posi. loading) (rad)	0.059	0.060	0.058	0.016	0.019	0.060
deformation capacity(*) (nega. loading) (rad)	-0.060	-0.040	-0.060	-0.015	-0.019	-0.060
residual axial load capacity (kN)	883	238	320	219	287	853
residual axial load capacity ratio (**)	0.74	0.20	0.27	0.13	0.18	0.52

(* : loss point of design lateral load defined as point where restoring force degrade to 80% of maximum strength)
(** : residual axial loading capacity/$bD\sigma_B$)

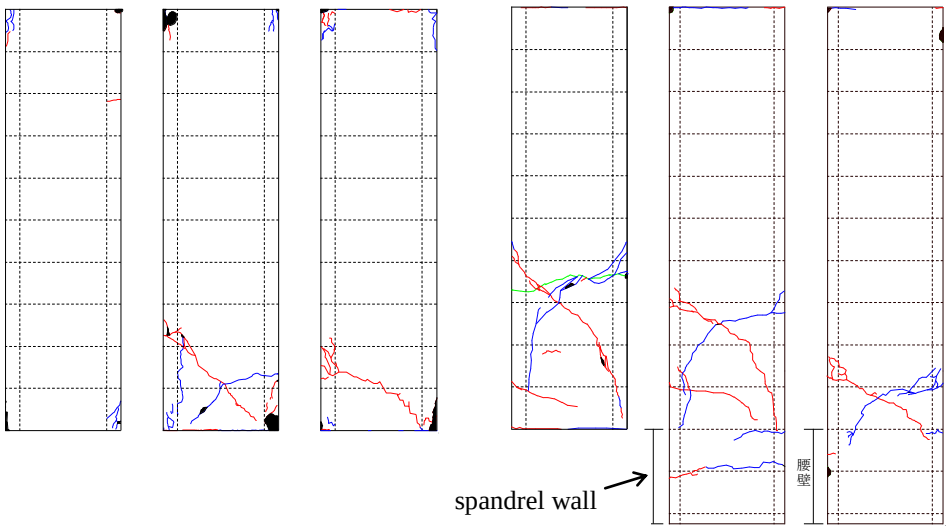

(a)SIM-0 (b)SIM-S (c)SIM-L (d)SIM-LL (e)SIM-LL-k (f)SIM-SS-k

Figure 3.1. Crack patterns at maximum strength

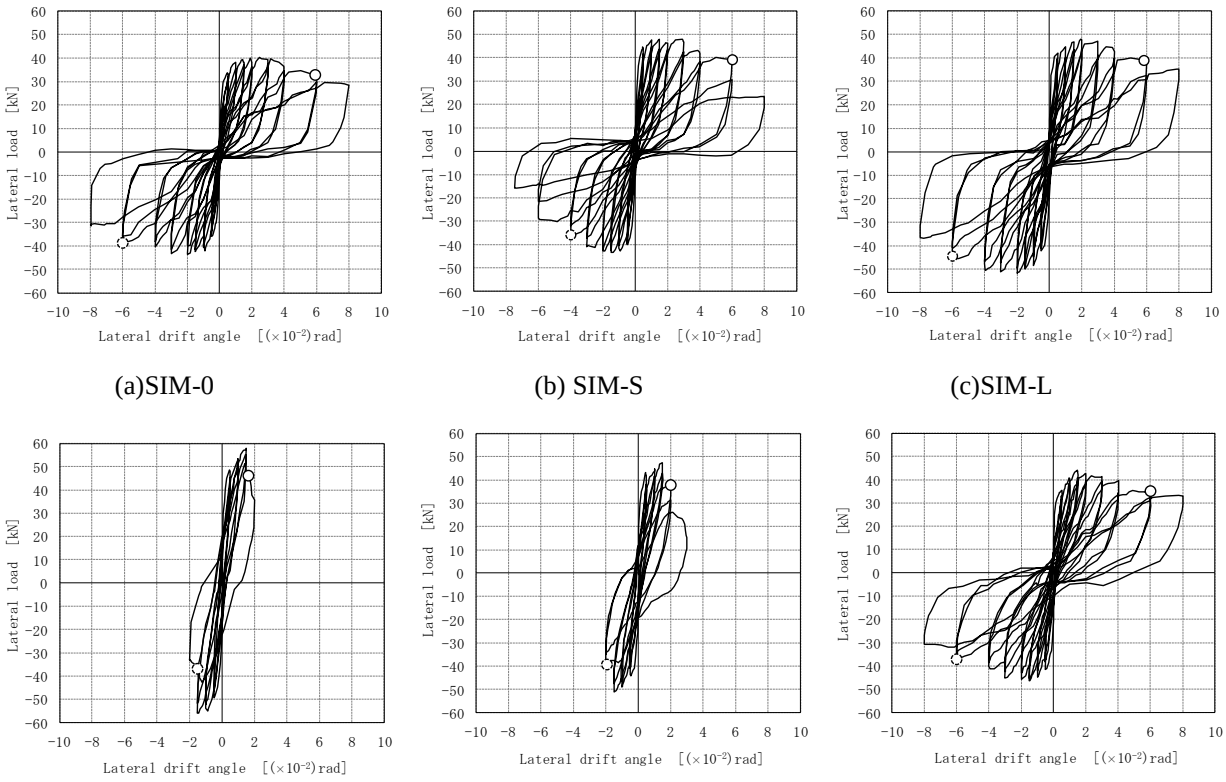

(a)SIM-0 (b) SIM-S (c)SIM-L

(d)SIM-LL (e) SIM-LL-k (f)SIM-SS-k

Figure 3.2. Lateral load – lateral drift angle relationship (○loss point of design lateral load defined as point where restoring force degraded to 80% of maximum strength)

4. EFFECTS OF CUT OFF BARS AND SPANDREL WALLS

Figure 4.1(a)~(c) compare envelope curves of lateral load- lateral drift angle relationship. Note that in these figures horizontal axis represents story drift angle converted from member drift angle according to Eq. (1).

$$R_{story} = \frac{h_o}{H} \cdot R_{mem} = \frac{2}{3.7} \cdot R_{mem} \quad (1)$$

Where, h_0 is the inner height of the column, H is the height of the story, R_{mem} is the drift angle of the member, R_{story} is the converted drift angle of the story.

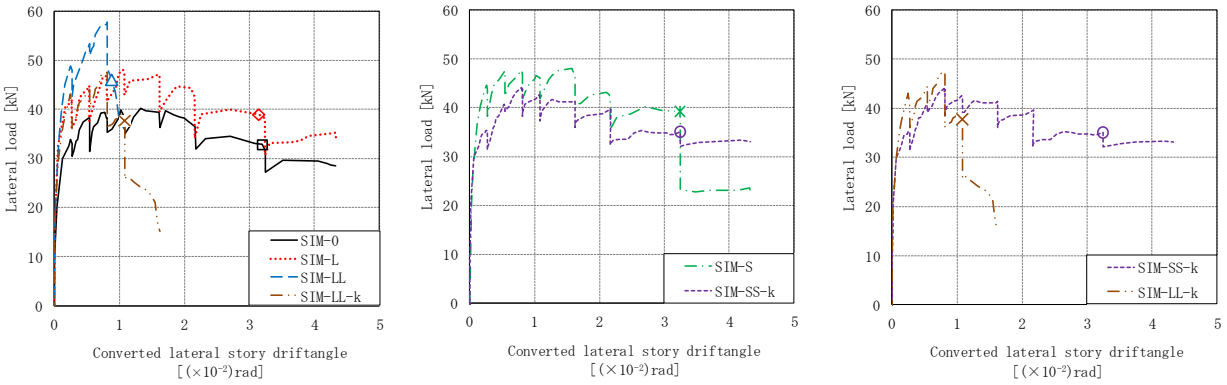

(a)SIM-0,L,LL,LL-k (b) SIM-S,SS-k (c)SIM-SS-k,LL-k

Figure 4.1. Comparison of envelope curve (○□◇×※loss point of design lateral load defined as point where restoring force degraded to 80% of maximum strength)

4.1 Effects of hinge location of longitudinal reinforcement

Comparison between specimens SIM-L and SIM-LL in Figure 4.1(a) shows that the deformation capacity of SIM-LL was much worse comparing to SIM-L which showed almost same favorable deformation capacity as SIM-0 without cut off bars. This was cause by the difference of yielding hinge locations of longitudinal reinforcement. The yielding hinge location of SIM-L with small amount of cut off bars neglecting β bars was the bottom of the column although that of SIM-LL with large amount of cut off bars considering β bars was the cut off point of the column. The width of diagonal crack generated at the cut off point became wide in case of SIM-LL, which lead to the deterioration of shear resistance between the surfaces of diagonal cracks. Although the width of diagonal crack did not become wide n case of SIM-L because the bottom of the column yielded. And this is the reason of the difference of deformation capacities.

4.2 Effects of presence of spandrel walls

Comparison between specimens SIM-LL and SIM-LL-k in Figure 4.1(a) shows that the deformation capacities of these two specimens were comparable and very small, which means that the effect of presence of spandrel walls on deformation capacities was small. However the maximum strength of specimen SIM-LL without spandrel walls was a little bit larger than that of specimen SIM-LL-k with spandrel walls, which means that the presence of spandrel walls reduced the flexural strength. This can be explained by the substantial inner height (h_0) of the column became longer due to the lack of confining effect by thin spandrel walls.

Comparison between specimens SIM-S and SIM-SS-k in Figure 4.1(b) shows that the relationship between these two specimens were almost same as that between SIM-LL and SIM-LL-k in Figure 4.1(a). Namely deformation capacities of these two specimens were comparable and very small and the maximum strength of specimen SIM-S without spandrel walls was a little bit larger than that of specimen SIM-SS-k with spandrel walls.

4.3 Effects of length of cut off bars

Comparison between specimens SIM-SS-k and SIM-LL-k in Figure 4.1(c) shows the effect of length of cut off bars. Note that the yielding hinge locations of these two specimens were the cut off point of the column. The deformation capacity of specimen SIM-LL-k with long cut off bars was much worse comparing to SIM-SS-k which showed almost same favorable deformation capacity as SIM-0 without cut off bars. This can be explained by the difference of inclination angle of diagonal cracks generated from the cut off point. The inclination angle of the diagonal crack of specimen SIM-LL-k was approximately 50~60 degree, in which case the shear deterioration between crack surface lead to a significant shear strength degradation of the column. On the other hand the inclination angle of diagonal crack of specimen SIM-SS-k was approximately 25 degree, in which case the shear deterioration between crack surface did not lead to a significant shear strength degradation of the column.

5. CONCLUING REMARKS

(1)Although the calculated failure mode is flexure, the deformation capacity of a column with cut off bars degrades tremendously on condition that the yielding hinge location is cut off point and the inclination angle of diagonal cracks generated from the cut off point is approximately 50~60 degree.
(2)The effect of presence of spandrel walls on deformation capacities is small. However the maximum strength of a column without spandrel walls is a little bit larger than that of a column with spandrel walls, which means that the presence of spandrel walls reduces the flexural strength.
(3)According to the conclusions (1) and (2) the failure mechanism of columns of S-building damaged during the 2007 Niigata Chuetsu-Oki earthquake can be explained.

REFERENCES

Architectural Institute of Japan (1994). AIJ Structural Design Guidelines for reinforced Concrete Buildings

The Japan Building Disaster Prevention Association (2001). Standard for Seismic Evaluation of Existing Reinforced Concrete Buildings

Nagahashi T., Kokubo T., Nakamura Y. and Kato D. (2009). Seismic Performance of a R/C School Building Suffered during the Chuetsu and Chuetsu Oki earthquake. Journal of Structural Engineering, Architectural Institute of Japan and Japan Society of Civil Engineering. Vol 55B , pp. 459-468.(in Japanese)

Daisuke Kato, Yudai Miyajima and Yukiko Nakamura (2009): Evaluating Method of Deformation at Losing Point of Axial Load Carrying Capacity of RC Columns, Journal of Asian Architecture and Building Engineering Vol.8(2009), No.2, pp.501-508

Daisuke Kato and Tetsuo Nagahashi (2011). Failure Mode of Columns of Existing R/C Building Damaged during the 2007 Niigata Chuetsu-Oki Earthquake, The Twelfth East Asia-Pacific Conference on Structural Engineering & Construction, Hong Kong SAR, China, 2011 January

Daisuke Kato and Yukiko Nakamura(2011): Effects of Loading Conditions and Hoop Details on Residual Axial Load Capacity of R/C Columns Failing in Shear, Journal of Asian Architecture and Building Engineering Vol.10(2011), No.2, November 15, pp.399-405